ELSEVIER

Chemical Engineering Journal 118 (2006) 107–118

Chemical Engineering Journal

www.elsevier.com/locate/cej

The effect of carbon dioxide on β-dicalcium silicate and Portland cement

Olga Shtepenko [a,*], Colin Hills [a], Adrian Brough [b], Mike Thomas [a]

[a] *Medway School of Science, University of Greenwich, United Kingdom*
[b] *Department of Civil Engineering, University of Leeds, United Kingdom*

Received 13 December 2005; received in revised form 3 February 2006; accepted 3 February 2006

Abstract

Carbonation of silicate-based minerals and industrial residues can help to reduce CO_2 emissions as well as produce useful materials. However, until a full understanding of the chemistry and microstructural development of carbonation products is obtained, their utilization in engineering applications may remain limited. In respect of this, the present work examines microstructural properties of accelerated carbonated dicalcium silicate and Portland cement by using the complementary analytical techniques of XRD, SEM, TG-DTA, and NMR MAS. It was found that carbon dioxide reacts with calcium silicates to form calcite and aragonite and a polymerized silicate product comprised of cross-linked Q^3 co-ordinated silicon and fully polymerized Q^4 co-ordinated silicon. The extent of silicate polymerization was higher in carbonated dicalcium silicate, however, in the Portland cement-derived product, Al substitution in the Si-framework was detected. The amount of CO_2 that reacted with dicalcium silicate and Portland cement was 48 and 37% by mass, respectively.

Keywords: Carbon dioxide sequestration; Accelerated carbonation; Anhydrous silicate minerals; Characterization

1. Introduction

In recent years there has been an increasing interest in the sequestration of industrial carbon dioxide by mineral carbonation [1–3]. Silicates and oxides of calcium and magnesium derived from both geological media and man-made processes have been considered as potentially effective sinks for CO_2 disposal.

As a natural mineral feedstock, earth silicates, including serpentine $Mg_3SiO_5(OH)_4$, wollastonite $CaSiO_3$ and olivine Mg_2SiO_4, have been identified as being both widely available and susceptible to carbonation [1,3]. However, the impact and cost of large-scale mining and pre-treatment of the rock media prior to carbonation may place restrictions on this approach [4].

Synthetic silicate-based materials, including industrial residues such as metallurgical slags, combustion ashes, and cement kiln dust, can be a sustainable alternative to natural silicates as they are often available in industrial areas close to CO_2 sources, precluding the need for mining and transportation, and some of them have better reactivity (i.e. available in fine powders) [1,2,5,6]. An additional major advantage is that certain properties of these materials can be altered by carbonation, reducing their environmental impact and increasing the value. For example, recycling of carbon dioxide in cement composites can reduce product setting time and enhance strength development [7,8]. Carbonation has been also used to stabilize metallurgical 'falling' slag containing unstable β-dicalcium silicate [5,6], and with combustion ashes the application of CO_2 has been used to improve both their physical stability and metal leaching properties [2,9].

Preliminary work involving accelerated carbonation of Portland cement powder resulted in carbonated products that were effective in removing heavy and radioactive metals from aqueous solution [10]. This investigation highlighted the potential of converting calcium silicate-based materials into low-cost sorbents whilst also utilizing CO_2 gas that would otherwise be emitted to the atmosphere. However, the structural properties of these 'sorbents' require further investigation if metal–sorbent interactions are to be fully understood.

A summary of work on the carbonation of a number of anhydrous calcium silicates is presented in Table 1; and shows that under different carbonation conditions, a decrease of Ca/Si ratios in original mineral matrices and formation of $CaCO_3$ have been observed [3,11–14]. However, the structure of transforming silicate phases is not fully understood, and has been reported to comprise amorphous silica [6,11]. Other studies describe a low-

* Corresponding author. Tel.: +44 1932577296; fax: +44 1932571917.
E-mail address: olga_shtepenko@hotmail.com (O. Shtepenko).

1385-8947/$ – see front matter © 2006 Elsevier B.V. All rights reserved.
doi:10.1016/j.cej.2006.02.005

Table 1
Structural studies on carbonated calcium silicates

Mineral phase [source]	Carbonation products	Conditions	Characterization techniques
Single silicate phases			
Dicalcium silicate, Ca_2SiO_4			
[11]	Amorphous silica gel, aragonite ($CaCO_3$)	T 20 °C; RH[a] 80%; P_{CO_2} 1 bar	XRD, SEM
[12]	Calcium silicate hydro-carbonate; aragonite	T 20 °C; RH 50%; CO_2 5%;	DT-TGA; XRD; Gas Spectr.
[13]	Low-lime C–S–H gel; calcite ($CaCO_3$)	T 20 °C; W/S[b] 0.125; RH 50%; P_{CO_2} 2 bar	XRD; SEM-XRF
[14]	Low-lime C–S–H gel; calcite; vaterite	T 20 °C; W/S 0.2; P_{CO_2} 0–56 bar	TGA; SEM; XRD
Tricalcium silicate, Ca_3SiO_5			
[11]	Amorphous silica gel, aragonite	T 20 °C; RH 80%; P_{CO_2} 1 bar	XRD, SEM
[12]	Calcium silicate hydro-carbonate; calcite	T 20 °C; RH 50%; CO_2 5%;	DT-TGA; XRD; Gas Spectr.
[13]	Low-lime C–S–H gel; calcite	T 20 °C; W/S 0.125; RH 50%; P_{CO_2} 2 bar	XRD; SEM-XRF
Wollastonite, $CaSiO_3$ [14]	Low-lime C–S–H gel; calcite	T 20 °C; W/S 0.2; P_{CO_2} 0–56 bar	TGA; SEM; XRD
Multi-component silicate phases			
Portland cement [7]	$CaCO_3$	T 20 °C; W/S 0.125	XRD, TGA
Slag containing Ca_2SiO_4			
[5]	Calcite	T 20 °C; W/S 0.125 P_{CO_2} 3 bar	XRD; SEM
[6]	$CaCO_3$; Ca-containing SiO_2	T 100 °C; W/S 10; P_{CO_2} 20	XRD, SEM

[a] RH, relative humidity maintained during carbonation.
[b] W/S, the ratio of water added to anhydrous mineral powder prior to carbonation.

lime silica gel (C–S–H) in which calcium is bound with silicate units [7,13,14], whereas Goto et al. [12] argued for the formation of calcium silicate hydrocarbonate. Little information on the structure of Si-rich carbonation products can be found from the research involving magnesium silicates [1,15].

The present work seeks to address these uncertainties through an investigation of carbonated products of β-dicalcium silicate and anhydrous Portland cement using a range of complementary analytical techniques, including NMR spectroscopy; which is a proven method for the investigation of silicate structures.

1.1. Approach

The way in which accelerated carbonation is applied to calcium silicate minerals may have a considerable bearing on the rate of reaction and nature of the carbonated products. The rate of atmospheric carbonation is generally too slow to be used on an industrial scale, but when the reaction rate is enhanced sufficiently, for example, by using aqueous processes, the industrial-scale sequestration may be considered feasible [1,5,11–14].

During aqueous carbonation, CO_2 rapidly reacts with calcium silicate in the presence of water or water vapour. However, when most of mineral surface has reacted, a continuous layer of carbonation products acts as a barrier to the two-way diffusion and hinders the reaction [2,11,15]. In order to mitigate the inhibiting effect of this passivating layer, different approaches have been suggested [1], including raised temperatures and pressures, mechanical activation and the use of chemical accelerators and additives, such as $NaHCO_3$, NaCl, and acid.

The use of mechanical activation (i.e. grinding) has several advantages over other methods. The process is technically simple, does not involve chemicals, and most importantly, can increase carbonation efficiency by an order of magnitude [15–17]. In view of this, mechanical activation approach is adopted in the present work and is described below.

2. Experimental

2.1. Materials

The materials used in this study were dicalcium silicate (C_2S) and Portland cement (PC) comprised of tricalcium and dicalcium silicates and minor quantities of tricalcium aluminate and tetracalcium aluminoferrite.

Portland cement (reference batch TG1/12) was supplied by Blue Circle Cement. Beta-dicalcium silicate (β-C_2S) was prepared by grinding a 2:1 molar ratio mixture of reagent-grade lime and silica and small amounts of MgO and Al_2O_3 [18]. The mixture was then pelletised and sintered at 1450–1500 °C. The composition of both materials is given in Table 2.

Table 2
Oxide composition of Portland cement and dicalcium silicate

Material	Constituent (%)								
	CaO	SiO_2	Al_2O_3	Fe_2O_3	MgO	K_2O	Na_2O	SO_3	LOI
PC	64.1	20.5	4.8	2.8	1.0	0.66	0.12	3.1	1.6
C_2S	63.9	33.9	0.12	0.11	0.46	0	0	0.04	1

Fig. 1. Carbonation chamber equipped with a CO_2 pressure control mechanism.

2.2. Methods

The two materials under investigation were mixed with 10% of de-ionized water (water/solid ratio = 0.1) and placed immediately into a carbonation chamber (Fig. 1), to be purged with pure CO_2 at the pressure of 2 bar for 60 min. The materials were then dried at 40 °C and ground in a ball mill for 2–3 min. This procedure was repeated five times until analysis by XRD revealed that the intensity of X-rays from the unreacted phases had fallen to the background level (Figs. 2 and 3). The carbonated samples were then finally dried at 40 °C, sealed in polyethylene bags and stored in a desiccator.

Semi-quantitative X-ray powder diffraction (Siemens D500 X-ray diffractometer) was carried out using Cu Kα radiation between 10° and 60° 2-theta, with a step-rate of 0.01° s^{-1}. Scanning electron microscopic analysis of polished, resin impregnated specimens, utilized a JEOL JSM-53C microscope with a LINK 860 energy dispersive X-ray (EDX) system and an accelerating voltage of 20 kV.

^{29}Si and ^{27}Al solid-state nuclear magnetic resonance (NMR) spectroscopy was used to investigate the structure of both crystalline and amorphous phases. ^{29}Si and ^{27}Al spectra were acquired at 59.5 and 78.20 MHz, respectively, using a Varian Infinity Plus 300 spectrometer equipped with an Oxford Instruments 7.05 T superconducting solenoid, and Chemagnetics MAS probes. Samples were spun at 4 and 10 kHz in 6 and 4 mm zirconia rotors for ^{29}Si and ^{27}Al analysis, respectively. The ^{29}Si spectra were excited with a 45° pulse, with a pulse delay of 5 s and acquired directly. The ^{1}H–^{29}Si cross-polarization (CP) spectra were acquired using a Hartman-Hahn field strength of 40 kHz with contact time of 3 ms. ^{27}Al MAS NMR spectra were acquired with a pulse delay of 1 s, and a short excitation pulse to ensure uniform excitation.

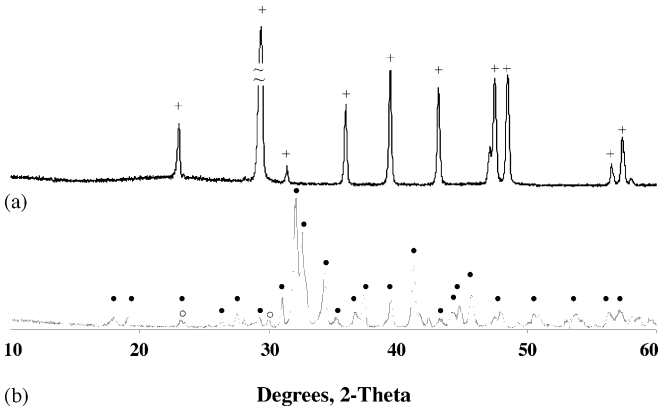

Fig. 2. X-ray diffraction patterns of (a) synthesised C_2S and (b) carbonated C_2S. Mineral phases depicted include: (+) calcite, (●) dicalcium silicate (Ca_2SiO_4), and (◯) wollastonite ($CaSiO_3$).

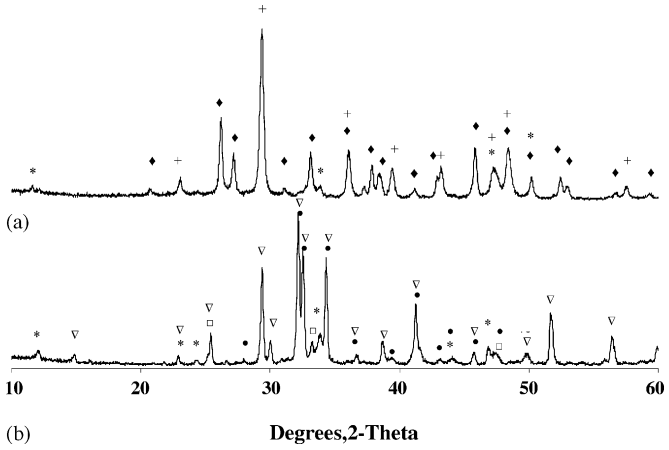

Fig. 3. X-ray diffraction patterns of (a) PC and (b) carbonated PC. Mineral phases depicted include: (♦) aragonite, (+) calcite, (●) dicalcium silicate (Ca_2SiO_4), (▽) tricalcium silicate Ca_3SiO_5, (□) tricalcium aluminate ($Ca_3Al_2O_6$), and (*) calcium aluminium iron oxide (C_4AF).

Carbon dioxide uptake by parent materials was evaluated with Stanton Redcroft STA 780 Simultaneous Thermal Analyzer. Samples weighing 20 mg were packed into a ceramic crucible, and then heated in air (flow rate of 10 °C min^{-1}) from 20 to 1000 °C, using an alumina reference material.

3. Results

3.1. Mineralogical composition

The examination of carbonated materials by XRD gave reflections for calcite and aragonite (Figs. 2 and 3), with aragonite being only detected in the carbonated PC. This data is generally consistent with previous studies [11–14], which show that the polymorphism of calcium carbonate may vary in similar mineral systems, and is a function of physical conditions (temperature, water content, etc.) and pore solution chemistry [23] at the time of formation. It is interesting to note that the carbonation of calcium silicates under high relative humidity and no added water resulted in the preferential formation of aragonite [11,12], whereas, with added water, calcite was formed [13,14].

The moisture content used in present work was kept nominally the same (10%), however, it is possible that it varied as result of the drying effect from the heat of carbonation, which although not measured here, is known to elevate materials temperatures by as much as 60 °C. Nevertheless, calcite was present in both carbonated materials examined, and it is certain that fac-

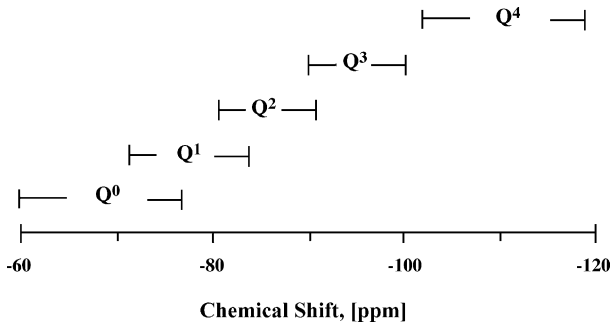

Fig. 4. Range of ^{29}Si chemical shifts for Si tetrahedra with different polymerizations in Al-free silicate phases.

tors favouring the formation of aragonite in carbonated PC were present.

Calcium aluminoferrite was also identified in carbonated PC, indicating its low reactivity to CO_2. The absence of any reflections for crystalline silicates in both carbonated materials supports the observation that the Si-containing reaction products are amorphous in nature [5–7,11–14].

3.2. NMR analysis

Magic-angle spinning (MAS) NMR spectroscopy is a powerful method for the investigation of silicates and aluminosilicate solid materials as it allows the identification of ^{29}Si and ^{27}Al structural environments, in both crystalline and amorphous phases [19,20].

There are well known relationships between various structural parameters and ^{27}Al and ^{29}Si NMR chemical shifts. For both nuclides the first-order control on the chemical shifts is the nearest-neighbour (NN) atomic coordination, where increasing NN coordination is correlated to more shielded chemical shifts [20]. Tetrahedrally coordinated Al (Al(4)) has chemical shifts in the region from +50 to +85 ppm, whereas octahedrally coordinated Al (Al(6)) has chemical shifts in the range of +15 to −15 ppm. ^{29}Si in tetrahedral coordination is identified between −62 and −126 ppm.

There are also significant next-nearest atomic neighbour (NNN) effects [20]. For ^{29}Si, in silicates and aluminosilicates, there are a number of important correlations. The chemical shift becomes more shielded as the polymerization increases (Fig. 4) [19]. The polymerization is described by the standard Q^n notation, where superscript n indicates the number of bridging oxygens per tetrahedron. In addition, for framework and sheet silicates (Q^2–Q^4) the ^{29}Si chemical shift becomes slightly less shielded as the number of Al(4) NNN to a given Si-site increases. For example, chemical shift characteristic of Q^3 sites lies in the region of −95 to −103 ppm. Substitution of one silicon atom in this group with Al atom (Q^3 (1 Al)) results in less negative values, ranging from approximately −89 to −97 ppm, due to de-shielding [19].

The ^{29}Si MAS NMR spectra obtained in this study (Fig. 5) indicated that a significant change in silicon environment occurred as calcium silicates were exposed to CO_2. The original Q^0 (−71 ppm) arising from monomeric silicate groups, typical

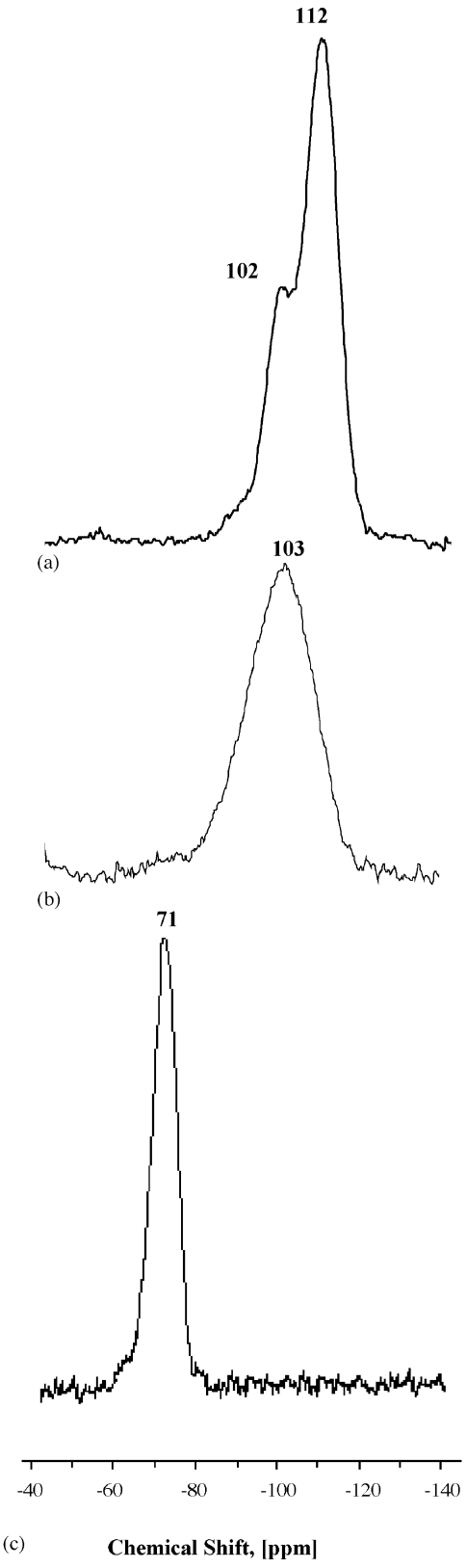

Fig. 5. ^{29}Si MAS NMR spectra of (a) carbonated C_2S, (b) carbonated PC, and (c) PC, acquired at 59.5 MHz and spinning speed of 4 kHz.

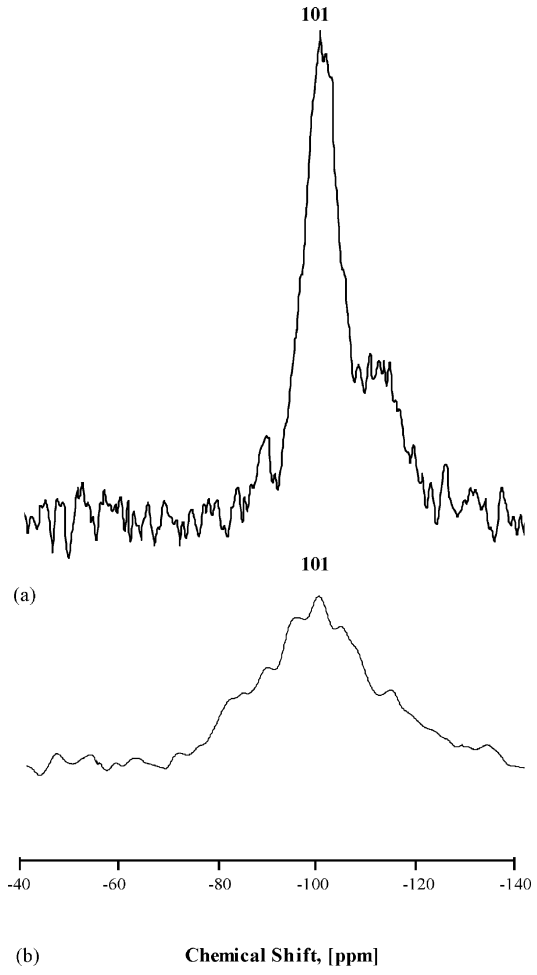

Fig. 6. ^{1}H–^{29}Si CPMAS NMR spectra of (a) carbonated C_2S and (b) carbonated PC, acquired at 40 kHz and contact time of 3 ms.

of C_2S and C_3S (Fig. 5c), were transformed into polymerized Q^3 and Q^4 arising from 3- and 4-coordinated silicate units (Fig. 5a and b). The predominance of fully polymerized silica phase could be observed from the resonance line centered at 112 ppm in the spectrum of carbonated C_2S (Fig. 5a). A distinct peak around 102 ppm was assigned to cross-linked silicate species.

In the spectrum of carbonated PC (Fig. 5b) a single broad resonance (−85 to −120 ppm) is indicative of a continuous range of $Q^{2–4}$ (0–1 Al) silicate units. A signal maximum at 103 ppm for the chemical shift distribution showed that silicate groups are primarily organized in three-dimensional networks of Q^3 (0–1 Al) and Q^4 (0–1 Al) silicate tetrahedra. A small amount of silicon was present as Q^2 units.

^{1}H cross-polarization combined with MAS (CPMAS) is a technique that enhances the signal from observed Si nuclei near protons, thus allowing sites in hydrated and anhydrous phases to be distinguished [20]. ^{29}Si–^{1}H spectrum of carbonated PC (Fig. 6b) exhibited poor signal/noise ratios and broad peak centered at 101 ppm, similar in shape to the ^{29}Si spectrum (Fig. 5b). This indicates that the whole range of $Q^{3–4}$ (0–1 Al) silicon sites contained some OH groups and/or water molecules in the immediate vicinity of silicon atoms. ^{29}Si–^{1}H spectrum of carbonated C_2S (Fig. 6a) had two easily resolved resonances at around 112 and 101 ppm. The intense resonance corresponding to Q^3 sites (101 ppm), indicated a predominant existence of hydrated phases within the three-dimensional silicate networks, rather than fully polymerized silica (Q^4).

The carbonated and non-carbonated samples of cement were further characterized by ^{27}Al MAS NMR spectroscopy to detect

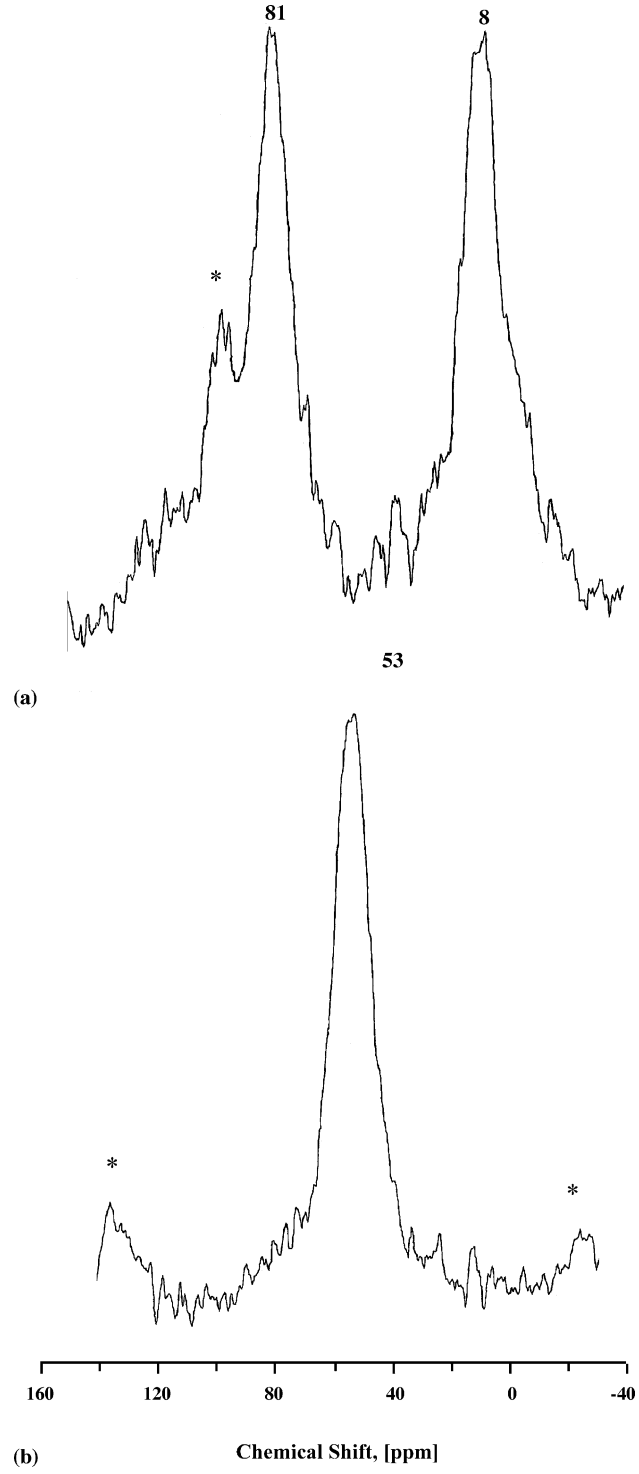

Fig. 7. ^{27}Al MAS NMR spectra of the central transitions for (a) PC and (b) carbonated PC, acquired at 78.2 MHz and spinning speed of 10kHz. Asterisks identify side bands.

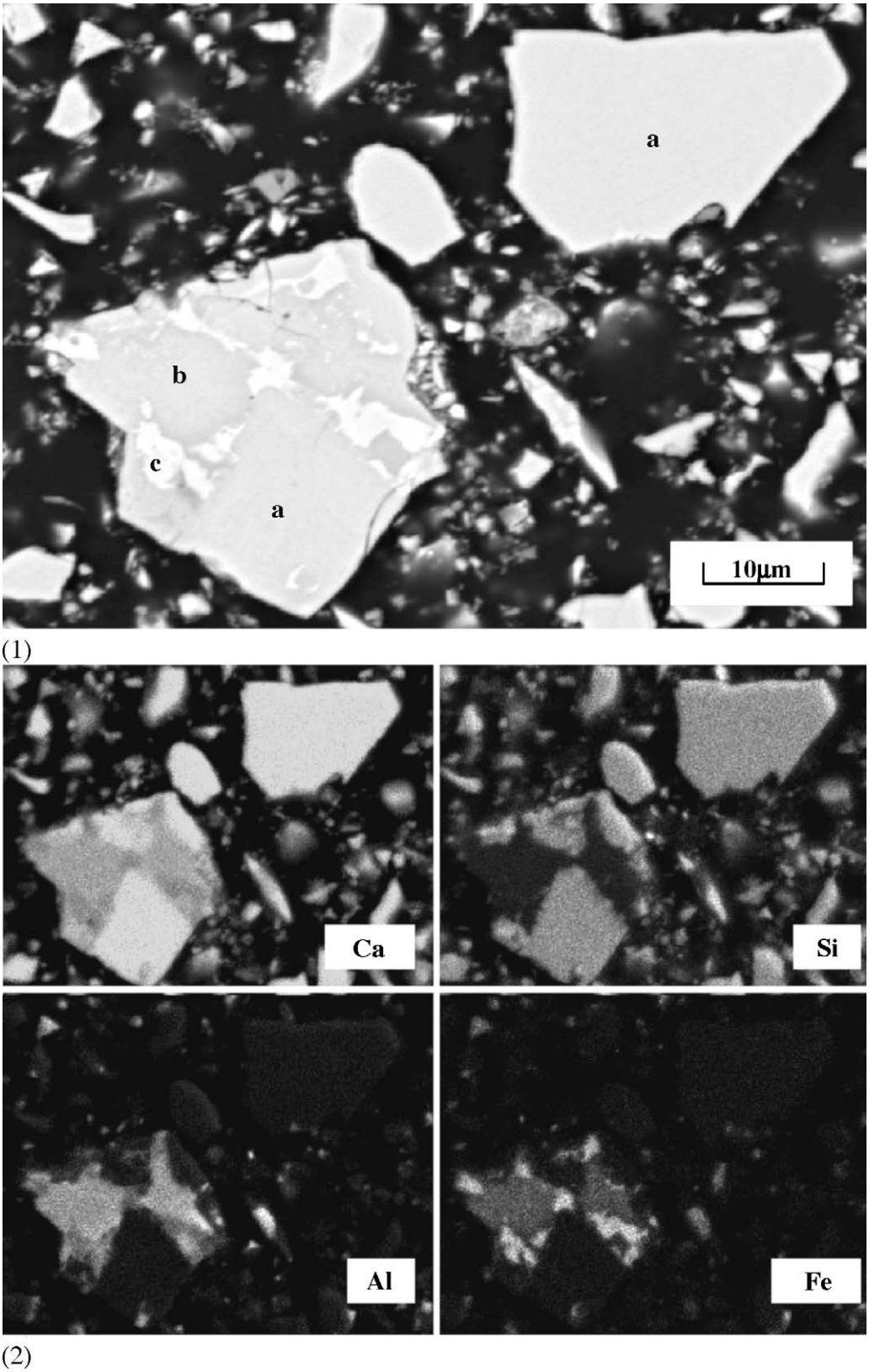

Fig. 8. (1) BSE image of polished PC particles, consisting of (a) C_3S and C_2S, (b) C_3A, and (c) C_4AF. (2) EDX element mapping micrographs for calcium, silicon, aluminium, and iron constituents.

the changes in the aluminium environment. The ^{27}Al spectrum of PC displayed two central transitions at around 81 and 8 ppm (Fig. 7a). The 81 ppm center-band was assigned to tetrahedrally coordinated aluminium sites (AlO_4) in C_3A, and Al-guest ions incorporated into C_2S and C_3S [20,21]. The center-band at 8 ppm demonstrated the presence of octahedrally coordinated aluminium (AlO_6), possibly originating from insignificant C_3A hydration [20]. In the carbonated sample the presence of different tetrahedral sites was observed at around 53 ppm (Fig. 7b). This was not in the region expected for aluminium substituted into C–S–H (approximately 70 ppm [20]), but in the region expected for aluminium substituted into a cross-linked silicate network, such as a silica gel or zeolite [19]. This confirms that aluminium ions re-speciated in the process of carbonation as a result of C_3A decomposition, and substituted some silicon in the formed Q^3 and Q^4 silicate networks. It should be noted that Al present in the ferrite phase, C_4AF, was largely not observed, as it is well established that aluminium present in paramagnetic phases contributes little or not at all to ^{27}Al spectra [22].

3.3. SEM observations and microanalysis

Backscattered electron imaging of the PC (Fig. 8(1)) showed ferrite (C_4AF), the bright interstitial phase, labelled 'c', alite and belite (C_3S and C_2S, respectively), labelled 'a', and aluminate (C_3A), labelled 'b'. Element maps for Ca, Si, Al, and Fe are shown in Fig. 8(2); the images obtained from the β-C_2S are not included.

The micrographs obtained from the carbonated materials (Figs. 9 and 10) show that the morphology of calcium silicates substantially changed after reacting with CO_2. Three main phases were identified, comprising a decalcified Si-rich pseudomorph, a Ca-rich phase, and unreacted aluminoferrite. The morphology of Ca-rich phase associated with carbonated C_2S

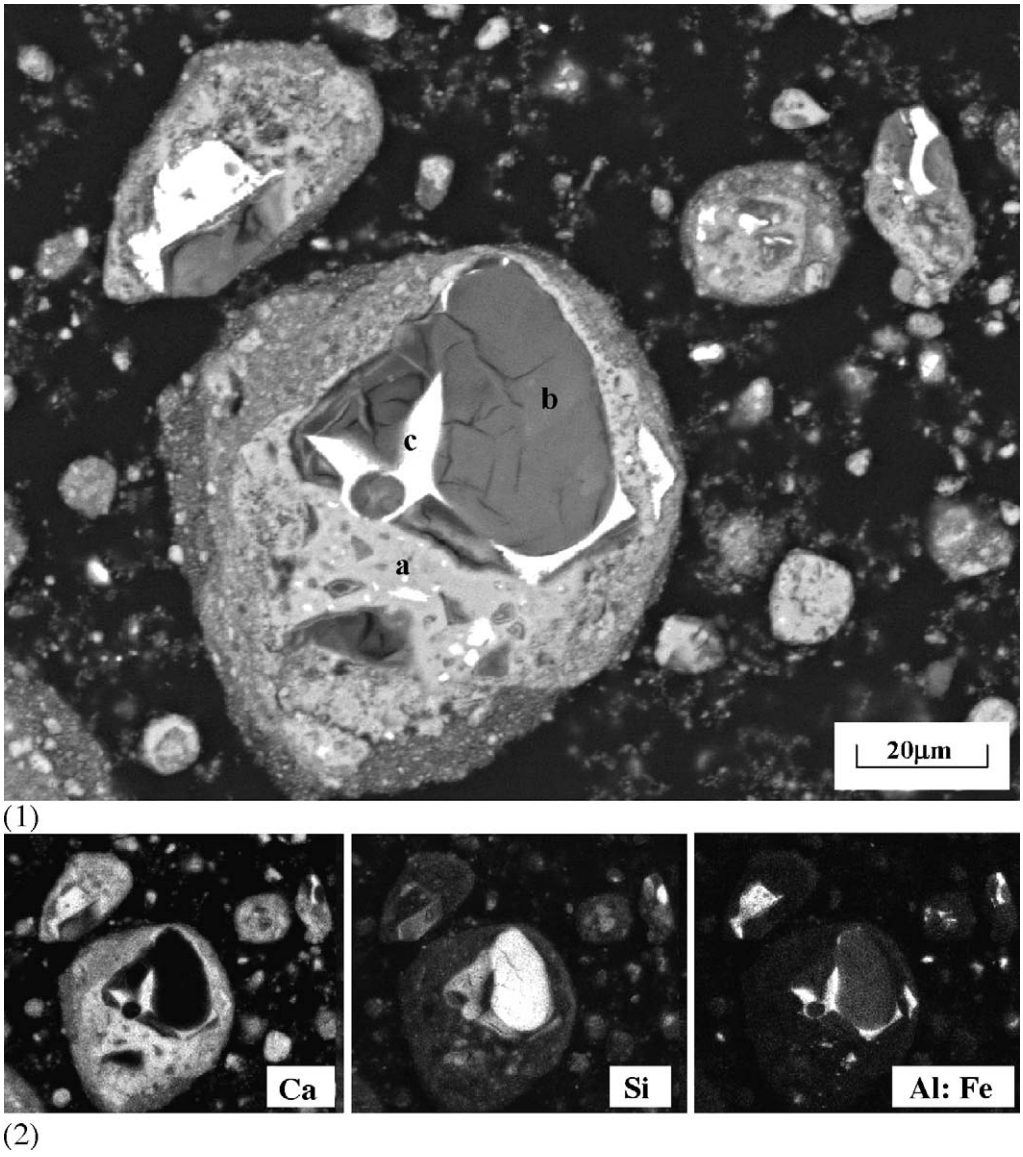

Fig. 9. (1) BSE image of carbonated PC, comprising (a) Ca-rich phase, (b) Si-rich phase, and (c) C_4AF. (2) EDX element mapping micrographs for calcium, silicon, aluminium, and iron (similar) constituents.

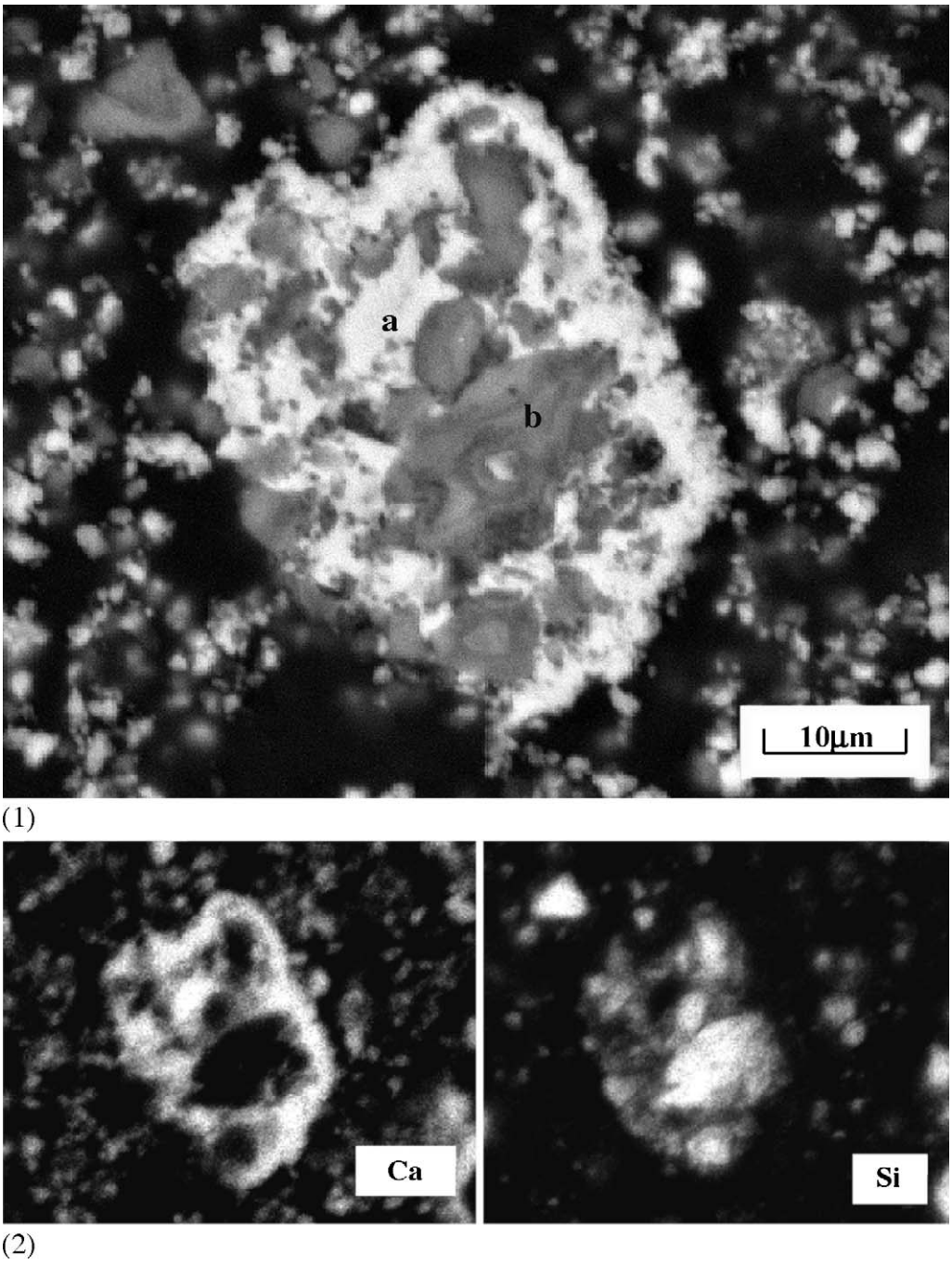

Fig. 10. (1) BSE image of carbonated C_2S, comprising (a) Ca-rich phase (b) Si-rich phase. (2) EDX element mapping micrographs for calcium and silicon constituents.

was different and appeared to have a porous "floc-like" structure. The particles of both carbonated products were irregular in size and shape.

EDX quantitative analysis of Ca, Si, Al, and Fe, involved the collection of X-ray counts from around 10 areas of each material (a total of ≈300 spots were analyzed), showed that in the Ca-rich product (labelled 'a') the Ca/Si ratios varied from 5 to 21. The Ca/Si ratios obtained from the examination of Si-rich phase (labelled 'b'), are given in Figs. 11 and 12, and demonstrate a higher proportion of low Ca/Si ratios (<0.1) in the carbonated C_2S, as might be expected from the higher degree of Si polymerisation. Overall, the Si-rich phases in both materials were characterized by Ca/Si ratios typically varying between 0.03 and 0.4.

In the carbonated cement Al was found in the Si-rich product, and calculated atomic Al/Si ratios varied from 0.04 to 0.1 (Fig. 12). This is consistent with the NMR results, which indicated the presence of aluminium-substituted silicate species. The composition and morphology of C_4AF appeared unaffected by accelerated carbonation.

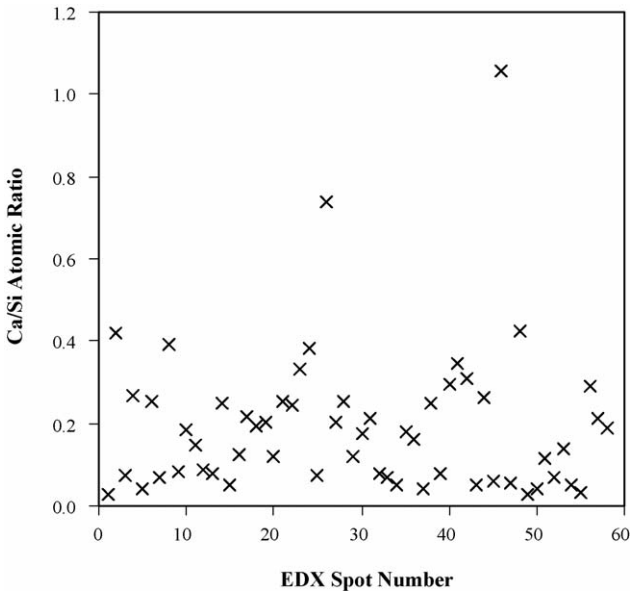

Fig. 11. Compositional variation of the Si-rich phase in carbonated C_2S.

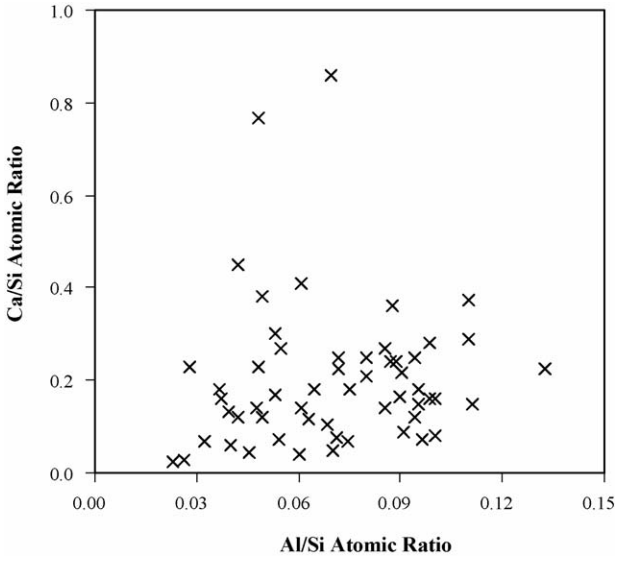

Fig. 12. Compositional variation of the Si-rich phase in carbonated PC.

3.4. Thermal analysis TG-DTA

The TG-DTA output for the carbonated samples is shown in Figs. 13 and 14 and the weight losses are summarized in Table 3.

Table 3
Thermal decomposition of the carbonated materials: calculated mass loss

Temperature range (°C)	Mass loss (%)	
	Carbonated C_2S	Carbonated PC
0–200	2.1	3.4
200–500	1	2.1
500–700	3.6	6.4
700–900	28.2	18.5
0–1000	34.7	30.5

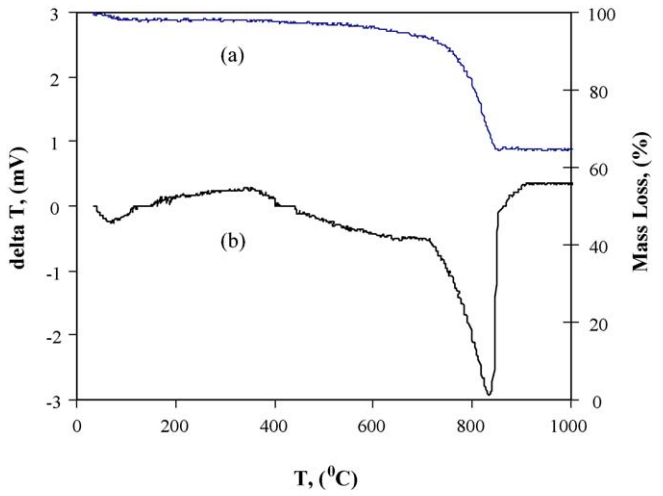

Fig. 13. (a) TG and (b) DTA curves of carbonated C_2S, obtained in air flow at a heating rate of 10 °C/min.

Both carbonated materials were characterized by endothermic peaks in the low temperature region. The endotherm for carbonated C_2S had a minimum at 80 °C and was accompanied by a small mass loss. The corresponding endotherm for carbonated PC had a higher temperature peak at 138 °C, and a greater mass loss, suggesting larger amount of physically bound water. A further small weight loss, in the region of 200–500 °C, was assigned to surface de-hydroxylation.

For both carbonated materials weight loss was observed between 500 and 700 °C followed by an endothermic peak, characteristic of $CaCO_3$ decomposition. The study by Goto et al. [12] has employed XRD, and TG-DTA in combination with gas-phase mass spectroscopy to identify the products of C_2S and C_3S carbonation. In addition to the mass loss associated with $CaCO_3$ decomposition, the authors recorded a mass loss between 500 and 600 °C and ascribed it to the decomposition of amorphous calcium silicate hydrocarbonate based on a correlated evolution of H_2O and CO_2. Without the gas analysis our results provide no direct evidence that calcium silicate hydrocarbonate is present in the carbonated C_2S and PC. However,

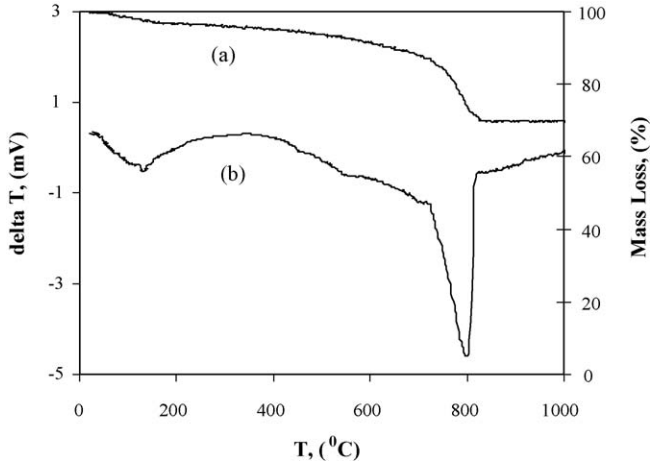

Fig. 14. (a) TG and (b) DTA curves of carbonated PC, obtained in air flow at a heating rate of 10 °C/min.

MAS NMR analysis identified cross-linked calcium silicates as the carbonation products of both C_2S and PC, thus it is possible that calcium end-members of Si framework reacted with carbon dioxide and water to form calcium silicate (hydro)-carbonates of varying stoichiometry.

Overall, the carbonated materials underwent four distinguishable mass losses, with the first two being due to dehydration and de-hydroxylation, followed by the losses associated with the low- and high-temperature de-carbonation reactions.

4. Discussion

4.1. Reaction products

The work described shows that during accelerated carbonation the calcium silicates substrates were transformed into new products. The ^{29}Si NMR data revealed that the silicate anions changed from single units to the three dimensional structures (see Fig. 15). The degree of polymerisation was substantially higher in the carbonated C_2S, and the intensities of distinct Q^4 and Q^3 peaks indicated that fully polymerised silica was predominant over the partially polymerised sites. A single broad resonance centered at 103 ppm was observed in the carbonated cement sample, giving the evidence of abundant cross-linked calcium silicate species (Q^3 sites) and some silica (Q^4 sites). It is probable that some of this structural calcium was also carbonated to form calcium silicate (hydro)-carbonates in addition to calcite and aragonite.

The differences in Si polymerization between the carbonated materials can be explained by the Ca/Si ratios of the starting substrates. When calcium reacts with carbon dioxide, calcium carbonate species nucleate on the surface of 'decalcified' silica matrix, in which silicon tetrahedra, being freed from calcium, combine to form chains, and then sheets as carbonation proceeds. When few or no calcium ions interfere with combining tetrahedra (in all directions), fully polymerised silica forms. It would be logical to conclude, therefore, that the carbonation of structurally similar calcium silicate minerals with lower Ca/Si ratios should result in a higher degree of Si polymerisation, and this is in agreement with the NMR results obtained during this work.

Another distinct feature of carbonated PC was the presence of Al in the polymerized Si product. ^{27}Al NMR showed that the original aluminate phase of PC decomposed, allowing aluminium to substitute for silicon in the Si-rich phase. The Al/Si ratios derived from quantitative SEM EDX microanalysis suggested that one aluminium atom was associated on average with 10–25 silicon atoms. Accordingly, it is reasonable to suggest that the carbonation of calcium silicate systems containing admixtures, for example, aluminate, may result in the incorporation of Al (or other constituents) into the polymerizing silicate framework.

The morphology of the samples examined by backscattered electron imaging suggested that Ca-rich and Si-rich phases were effectively separated in the carbonated products, and this was most likely due to grinding. The fact that unreacted ferrite was often found embedded in the polymerized Si-rich phase, underlines that this reaction product is pseudomorphic in nature.

4.2. Carbon dioxide uptake

The exposure of dicalcium silicate and cement powder to CO_2 and moisture produced a noticeable exothermic reaction which is described in previous work with anhydrous calcium silicates [7,11–14]; however in our work the amount of heat evolved was not measured. Nevertheless, a rapid temperature rise was observed over 10–20 min during the first two carbonation cycles. As the amount of CO_2 that reacts with calcium silicate appears to be a logarithmic function of time [7,12,14], this observation was not surprising.

The amount of CO_2 determined to have combined with the C_2S was 31.8% of the product's weight (see Table 3) and this corresponds to a CO_2 uptake of 48% of the weight of starting material; for PC this value was 37%. These figures equate to 480 and 370 kg of CO_2 captured per tonne of C_2S and PC, respectively.

The efficacy of carbonation was calculated with reference to Steinour's equation (1), which expresses theoretical sequestration potential of a material based on its stochiometry [24]:

$$CO_2\,(\%) = 0.785(CaO - 0.7SO_3) + 1.09Na_2O + 0.93K_2O \quad (1)$$

where CaO, SO_3, Na_2O, and K_2O are the mass percentages of relevant constituent oxides.

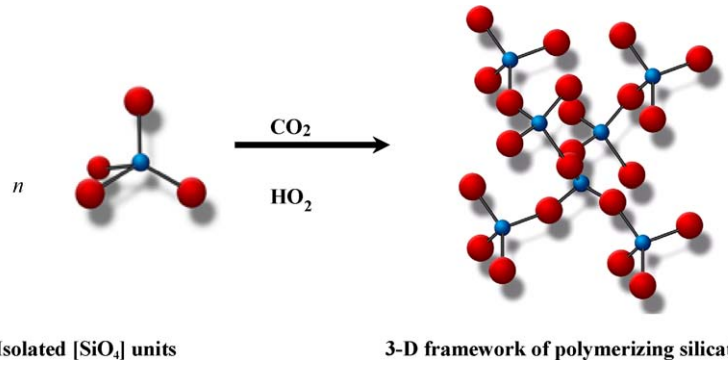

Fig. 15. Schematic illustration of silicon environment in calcium silicate systems before and after carbonation.

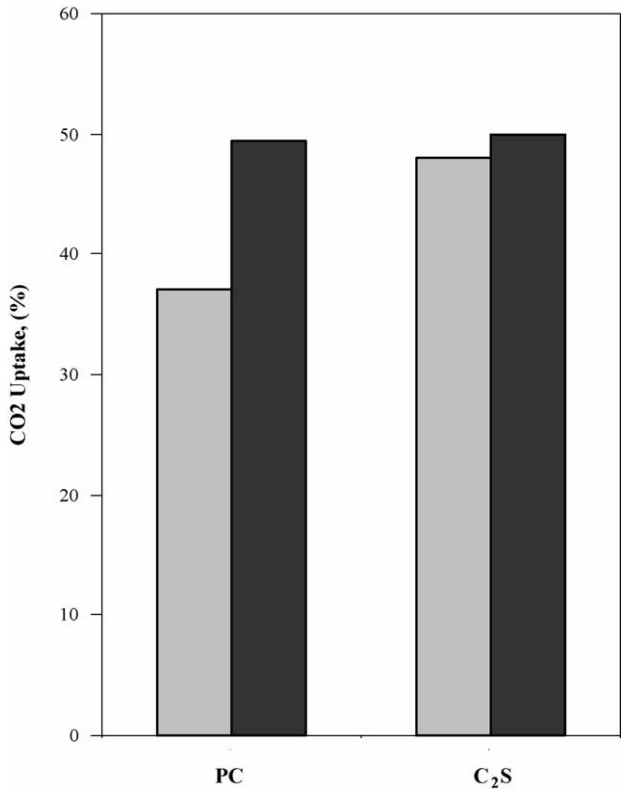

Fig. 16. Experimental CO_2 uptake (in grey) plotted against theoretical sequestration potential of C_2S and PC.

The calculated theoretical and experimental values for CO_2 uptake are presented in Fig. 16. It appears that carbonation was efficient and 96 and 75% of dicalcium silicate and Portland cement reacted with carbon dioxide, respectively. Other studies have reported up to 70% conversions of C_2S and C_3S when carbonated up to 24 h [12–14]. Wang et al. [7] achieved 7.3% conversion of cement powder at the W/S ratio of 1.25 after 30 min of carbonation. Clearly, the experimental conditions used in this study were more favourable and the use of mechanical activation and low W/S ratio were key to achieving the high CO_2 uptakes for the materials examined.

It is important to stress that although the theoretical value for CO_2 uptake can be calculated based on the stochiometry of a material, the actual CO_2 uptake is also reliant on mineralogy. For example, the calcium found in ferrite was not susceptible to carbonation, thus deducting from the theoretical sequestration potential of Portland cement.

5. Conclusions

A detailed structural examination of the carbonation products of β-dicalcium silicate and anhydrous Portland cement was carried out, and key structural differences in the reaction products were identified. These findings are summarized below:

- Both dicalcium silicate and Portland cement were transformed into new products on exposure to carbon dioxide. The original crystalline phases decomposed, with the exception of C_4AF in cement, and no crystalline silicate reaction products were detected. Calcite and aragonite were formed, and the latter polymorph was associated with carbonated PC.
- The structural environment of silicon in the carbonated products was identified by MAS NMR. Both cross-linked calcium silicate frameworks (Q^3 silicon environment) and fully polymerized silica (Q^4 silicon environment) were observed, with the latter being dominant in carbonated dicalcium silicate.
- The Ca/Si ratio of the parent material may influence the degree of silicate polymerization, as carbonated C_2S had higher proportion on silica (Q^4) in comparison to carbonated PC.
- The presence of certain admixtures can influence the chemistry of carbonation products. For example, the aluminate in Portland cement decomposed during carbonation resulting in aluminium being incorporated into polymerized silicate network.
- The PC and C_2S carbonated to 75 and 96%, respectively, of the maximum theoretical sequestration potential based on bulk chemistry. Mechanical activation was an important factor in achieving such high levels, suggesting that optimised carbonation conditions may not necessarily require raised temperatures and pressures.
- The chemistry and mineralogy of parent materials are primary controls on the effectiveness of carbonation. For example, the presence of Ca-bearing minerals such as calcium aluminoferrite may not readily combine with CO_2.
- The results of current work show that materials containing anhydrous calcium silicates have potential to capture significant quantities of CO_2. An equivalent of 480 and 370 kg of CO_2 was captured by each a tonne of C_2S and PC, respectively.

It is important to stress that the aim of current work was to broaden the knowledge on the structure of carbonation products of anhydrous silicate minerals which are either naturally available or produced by high temperature processes (i.e. constituents of slag, ash, cement powder). The carbonation of hydrated silicate systems, particularly hydrated cement-based materials has been described elsewhere [25–27]. The comparison of these two different classes of carbonated products indicates that silicate polymerization and formation of calcium carbonates are characteristic to both.

References

[1] W.J.J. Huijgen, R.N.J. Comans, Carbon Dioxide Sequestration by Mineral Carbonation: Literature Review, ECN Report ECN-C-03-016, Energy Research Centre of the Netherlands, 2003.
[2] D.J. Fauth, Y. Soong, C.M. White, Carbon sequestration utilizing industrial solid residues, Abstracts of Papers of the American Chemical Society, 223:030-Fuel Part 1, 2002.
[3] J.C. Wu, J.D. Sheen, S.Y. Chen, Y.C. Fan, Feasibility of CO_2 fixation via artificial rock weathering, Inst. Eng. Chem. Res. 40 (2001) 3902–3905.
[4] H. Herzog, Carbon Sequestration via Mineral Carbonation: Overview and Assessment, MIT Laboratory for Energy and the Environment, 2002.
[5] D.C. Johnson, C.L. MacLeod, P.J. Carey, C.D. Hills, Solidification of stainless steel slag by accelerated carbonation, Environ. Technol. 24 (6) (2003) 671–678.

[6] W.J.J. Huijgen, G.J. Witkamp, R.N.J. Comans, Mineral CO_2 sequestration in alkaline solid residues, in: Proceedings of the Seventh International Conference on Greenhouse Gas Control Technologies, Vancouver, Canada, 2004.
[7] A.S. Wang, D. Singh, L.J. Knox, Rapid setting of Portland cement by greenhouse carbon dioxide capture, in: Proceedings of the 96th Annual Meeting of the American Ceramic Society, Indianapolis, USA, 1994.
[8] A. Maries, C.D. Hills, Recycling carbon dioxide in the construction industry, in: International Conference on Technology Watch and Innovation in the Construction Industry, Brussels, Belgium, 2000.
[9] E. Rendek, G. Ducom, P. Germain, Carbon dioxide sequestration in municipal solid waste incinerator (MSWI) bottom ash, J. Hazard. Mater., in press.
[10] O.L. Shtepenko, C.D. Hills, N.J. Coleman, A. Brough, Characterization and preliminary assessment of a sorbent produced by accelerated mineral carbonation, Environ. Sci. Technol. 39 (1) (2005) 345–354.
[11] C.J. Goodbrake, J.F. Young, R.L. Berger, Reaction of γ-C_2S and C_3S with CO_2 and water vapor, J. Am. Ceram. Soc. 62 (1979) 168–171.
[12] S. Goto, K. Suenaga, T. Kado, Calcium silicate carbonation products, J. Am. Ceram. Soc. 78 (1995) 2867–2872.
[13] J.F. Young, R.L. Berger, J. Breese, Accelerated curing of compacted Ca silicate mortars on exposure to CO_2, J. Am. Ceram. Soc. 57 (1974) 394–397.
[14] J.M. Bukowski, R.L. Berger, Reactivity and strength development of CO_2 activated non-hydraulic calcium silicates, Cem. Conc. Res. 9 (1979) 57–68.
[15] M.J. McKelvy, H. Bearat, A.V.G. Chizmeshya, R. Nunez, R.W. Carpenter, Understanding Olivine CO_2 Mineral Sequestration Mechanisms at the Atomic Level: Optimizing Reaction Process Design: Technical Report, Arizona State University, USA, 2003.
[16] M.G. Nelson, Carbon Dioxide Sequestration by Mechano-Chemical Carbonation of Mineral Silicates: Technical Report, University of Utah, USA, 2004.
[17] W.K. O'Connor, D.C. Dahlin, D.N. Nilsen, et al., Continuing studies on direct aqueous mineral carbonation for CO_2 sequestration, in: 27th International Technical Conference on Coal Utilisation and Fuel Systems, Florida, USA, 2002.
[18] R. Berliner, C. Ball, P.B. West, Neutron powder diffraction investigation of model cement compounds, Cem. Conc. Res. 27 (4) (1997) 551–575.
[19] E. Gunter, M. Dieter, High-Resolution Solid-State NMR of Silicates and Zeolites, John Wiley and Sons, London, 1987.
[20] P. Colombet, A.R. Grimmer (Eds.), Application of NMR Spectroscopy to Cement Science, Breach Science Publishers, London, 1994.
[21] J. Skibsted, H.J. Jakobsen, C. Hall, Direct observation of aluminium guest ions in the silicate phases of cement minerals by Al-27 NMR-spectroscopy, J. Chem. Soc. Farday Trans. 90 (14) (1994) 2095–2098.
[22] J. Skibsted, H.J. Jakobsen, C. Hall, Quantitative aspects of ^{27}Al MAS NMR of calcium aluminoferrites, Adv. Cem. Bas. Mater. 7 (2) (1998) 57–59.
[23] R.J. Reeder (Ed.), Reviews in Mineralogy. Vol. 11: Carbonates: Mineralogy and Chemistry, Mineralogical Society of America, New York, 1983.
[24] H.H. Steinour, Some effects of carbon dioxide on mortars and concrete—discussion, J. Am. Concr. Inst. 30 (1959) 905–907.
[25] M. Fernández Bertos, S.J.R. Simons, C.D. Hills, P.J. Carey, A review of accelerated carbonation technology in the treatment of cement-based materials and sequestration of CO_2, J. Hazard. Mater. 112 (3) (2004) 193–205.
[26] S. Thomas, K. Meisegresch, W. Mullerwarmuth, I. Older, MAS NMR-studies of partially carbonated Portland-cement and tricalcium silicate pastes, J. Am. Ceram. Soc. 76 (8) (1993) 1998–2004.
[27] G.W. Groves, A. Brough, I.G. Richardson, C.M. Dobson, Progressive changes in the structure of hardened C_3S cement pastes due to carbonation, J. Am. Ceram. Soc. 74 (11) (2001) 2891–2896.